

# School of Physics and Astronomy



## An Introduction to Radio Interferometry and The Measurement Equation Formalism *Pedagogical Seminar*

Louise M. Ker  
March 2010

### Abstract

The next generation of radio telescopes, such as LOFAR, e-Merlin, ASKAP, MeerKat and eventually the SKA promise to open up the radio frequency range to unprecedented depth. Radio observations are highly relevant to almost every area of astrophysical study, yet the analysis of interferometric data is still perceived as being a specialised skill. In this seminar, I will introduce the basic concepts behind radio interferometry and aperture synthesis imaging, and latterly, the Measurement Equation formalism, currently being implemented in the next generation of radio interferometry data reduction software.

## Contents

<b>1</b>	<b>Introduction</b>	<b>3</b>
<b>2</b>	<b>Why Interferometry?</b>	<b>3</b>
<b>3</b>	<b>Some Basic Physics, and a Picture Based Introduction</b>	<b>4</b>
3.1	A Small Aside: Fourier Transforming Cats . . . . .	7
<b>4</b>	<b>The Radio Interferometry Problem: The Classical View</b>	<b>8</b>
<b>5</b>	<b>Spatial Coherence</b>	<b>10</b>
5.1	Aperture Synthesis . . . . .	11
5.2	Primary Beam . . . . .	12
5.3	Deconvolution . . . . .	12
<b>6</b>	<b>Calibration and Editing</b>	<b>13</b>
6.1	Self-Calibration . . . . .	13
<b>7</b>	<b>In Practice</b>	<b>14</b>
<b>8</b>	<b>The Measurement Equation</b>	<b>14</b>

## 1 Introduction

Radio interferometers constitute some of the world's most iconic telescopes, but the principles behind their operation are very different to those of a traditional single dish instrument. In this seminar, I will give the 'classical' introduction to radio interferometry, outlining the relevant maths and assumptions needed in analysing and imaging data from antenna array interferometers such as the VLA and GMRT. In the latter half I will introduce 'The Measurement Equation', a mathematically complete description of what is actually measured with any interferometer first introduced by Hamaker et al. (1996), and explain why this is basis is now essential for the next generation of new software based radio telescopes.

## 2 Why Interferometry?

To answer this, it is helpful to return to the basic requirements for any instrument used to observe astronomical sources at any wavelength. Good resolution and accurate intensity values, in other words, good signal to noise measures are essential for any science. An optical telescope measures the number of photons collected, and hence the signal to noise achievable depends on the diameter of the dish. A radio receiver measures the voltage induced by the radio signal received, and again, the wider the collecting area, the stronger the signal. Looking at the resolution however, classical optical diffraction theory limits the angular resolution achievable by a single dish telescope to

$$\theta \sim \frac{\lambda}{D} \quad (1)$$

where  $\lambda$  is the wavelength of the radiation received, and  $D$  is the diameter of the telescope. In the optical, a 6m dish provides  $\sim 0.025$  arcsec resolution (although in practice atmospheric seeing limits this), however a single radio dish observing at low frequencies can achieve at best only a few arcminutes resolution. For example, the FAST telescope currently being built in China, will be the largest single dish radio telescope in the world with a 500m dish diameter, and yet will only achieve a resolution of  $\sim 2$  arcminutes in the L band, (Zhao, 2009). Much of the desired science in radio astronomy relies on obtaining radio source positions with enough precision to enable cross-matching with data at other wavelengths. It was this initial poor resolution able to be achieved by the largest single dish long wavelength radio telescopes, that provided the initial motivation behind the development of radio interferometry.

*The very basic key concept behind an interferometer is that one can link many single radio dishes together, combining the signal received at each, and effectively simulating a large single radio telescope dish, with a diameter equivalent to the largest distance (baseline) between the smaller dishes.*

### 3 Some Basic Physics, and a Picture Based Introduction

Going back to the very beginning, a reminder of the experiment which first proved the wave nature of light, Young's Slits. A monochromatic source of light passing through two slits will diffract, and produce a fringe pattern of maxima and minima, an angular distance  $\lambda/d$  apart. The phase difference between waves will change as the path lengths taken vary, giving rise to the constructive & destructive interference seen on the viewing screen.

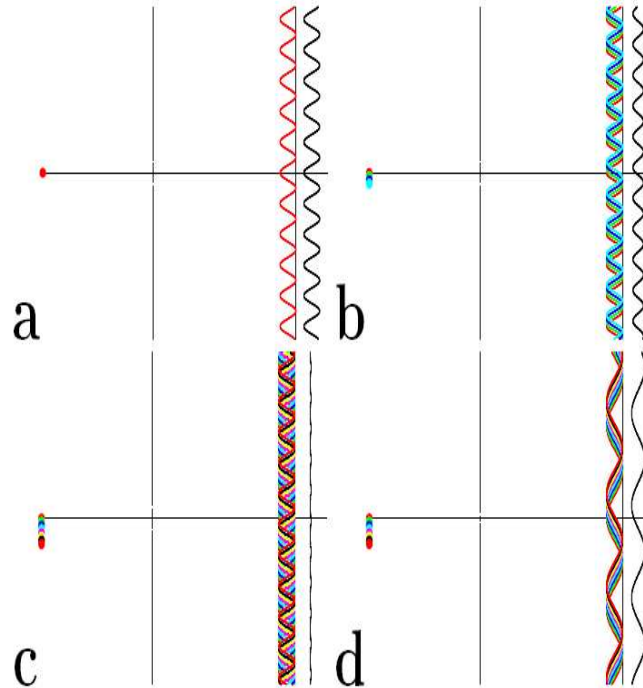


Figure 1: The Young's Slits experiment illustrated. Diagram credit Neal Jackson, (Jackson, 2004). Panel a) shows the basic experiment. b) What happens when the light source size increases? An angular shift in source position one way shifts the fringe patterns by the same amount the other. As the fringes come from a group of mutually incoherent sources, the intensity patterns add giving a reduced visibility. Panel c) shows what happens when the size of the source reaches  $\lambda/d$ , the fringes add to give zero visibility. Finally panel d) Shows that if the distance between the two slits is reduced, the same size of source is still able to give visible fringes.

Interferometers use exactly the same concept. First consider the simplest interferometer, composed of two antennas, as illustrated in figure 2. Everything we can learn about a source in the sky comes from the distribution of its electric field. Each antenna measures a different part of the wavefront arriving from the source. The signals from each antenna are cross-correlated, and analogous to the Young's slits experiments above, depending on the path taken and the distance between the antennas, the interferometer output will either be constructive or destructive. If we add in the Earth's rotation to this picture, one can imagine a source moving through the interferometer beam, giving positive and negative output, and producing a fringe pattern as in figures 3 and 4.

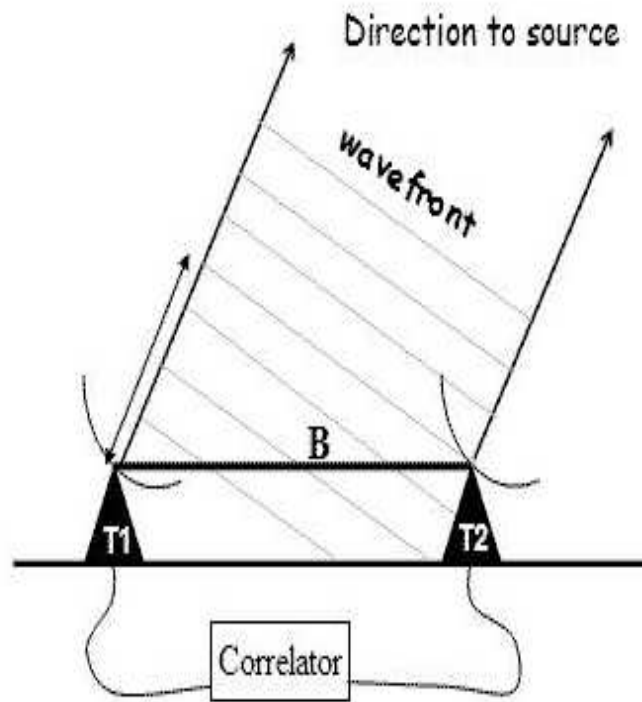


Figure 2: A very simple two element antenna interferometer. Image credit: David Brodrick, fringes.org

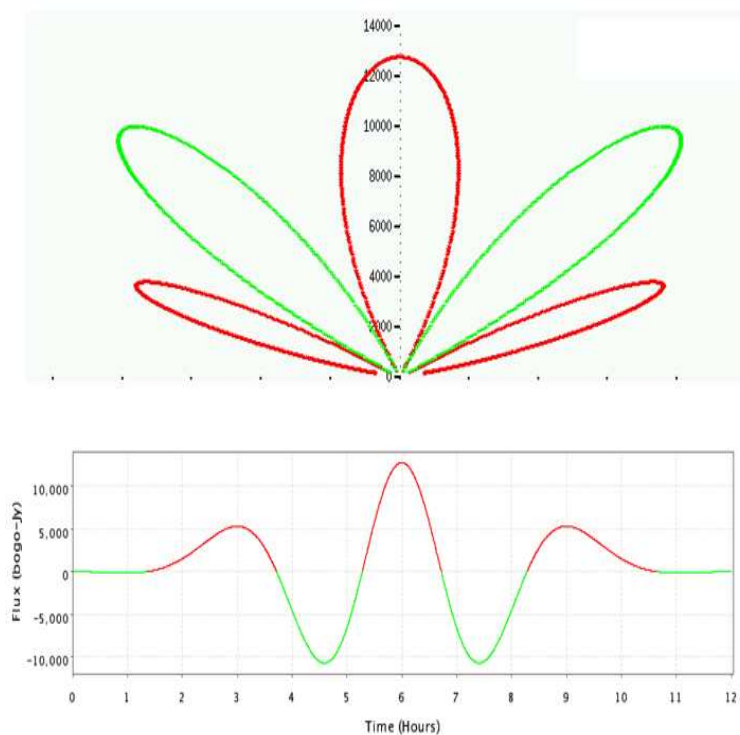


Figure 3: An illustration of the output of an interferometer. Green showing constructive interference, red destructive. The graph below is the output 'fringe pattern', more lobes appear when the baseline is longer. Image credit:David Brodrick, fringes.org

One obvious application of this fringe pattern, is to measure accurate radio source positions, and indeed this is what the very first interferometers were used for. It is also straightforward to measure the size of a source, by extending the size of the baseline until a weaker signal is received. This occurs when the angular size of the source becomes comparable to the distance between positive and negative lobes (see figure 4), which we know. Observations of extragalactic sources are made very much easier by this property, in that Galactic diffuse radio emission is generally ‘resolved out’ allowing background sources to appear. Some further useful properties of an interferometer include the fact that any internal instrument noise common to one antenna will not be present in the cross correlated signal, as noise is generally not coherent.

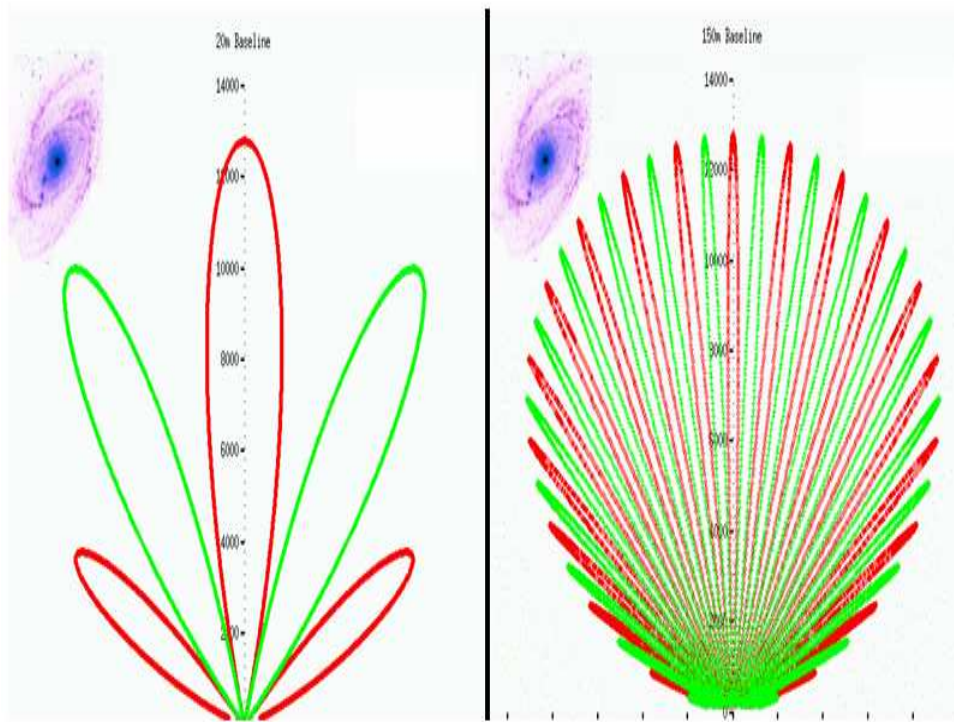


Figure 4: An illustration of how differing baseline length allows the interferometer to see different sized sources. Left is a short baseline, right a long baseline. For the short, as the galaxy moves through the beam it will either occupy a positive or negative lobe. However for the long, regardless of where the source is on the sky it will occupy both positive and negative lobes, and will not give a strong signal with the interferometer. In interferometry jargon, the source has become ‘resolved’. Image credit:David Brodrick, fringes.org

Figure 5 plots the intensity vs angular distance, visibility vs baseline length for a source. These two values, the intensity and the visibility are a Fourier Transform pair, and from the measured visibilities across an area of sky, we can derive the intensities.

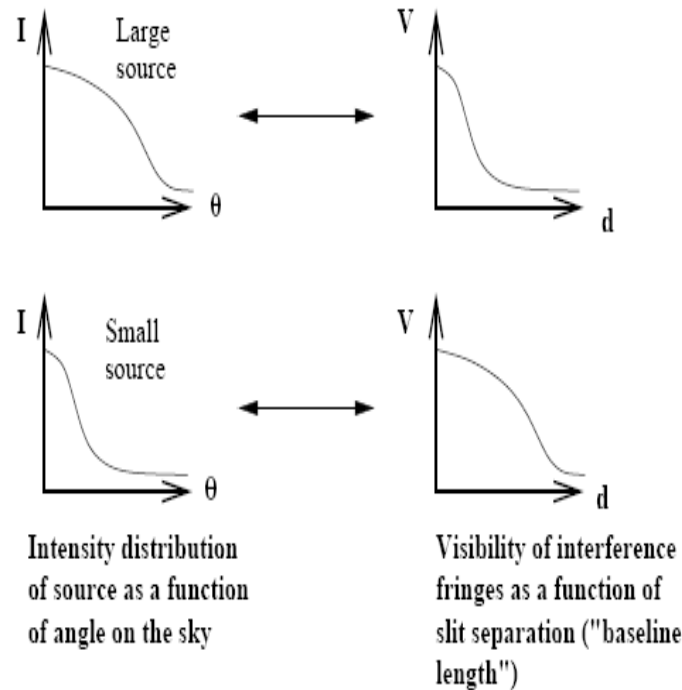


Figure 5: Relation between source brightness as a function of angular distance and visibility of interference fringes as a function of baseline length. Image credit: Neal Jackson, (Jackson, 2004).

### 3.1 A Small Aside: Fourier Transforming Cats

So far, the basic outputs of an interferometer have been discussed, but how does one go about making images from interferometric visibilities, and understanding them? For the maths, see the next section. For now let's have a think about Fourier transforming images. Visibilities are complex values, and so have an amplitude and a phase associated with each one. How do these contribute in the image plane? Very simply, the amplitude of a visibility affects the measured intensity in the image plane, and the phase, the position of the emission in the image plane.<sup>1</sup>

<sup>1</sup>The Virtual Radio Interferometer at <http://www.merlin.ac.uk/nam/vri.html> is a good way of visualising imaging and Fourier transforms in practice.

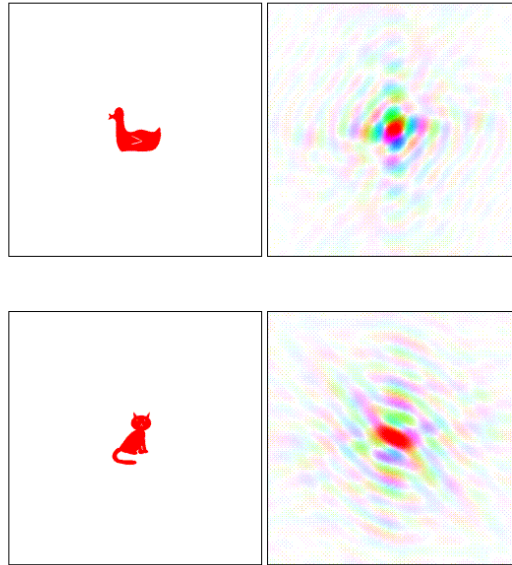


Figure 6: What really happens when you Fourier transform a cat. Image Credit Keith Cowtan <http://www.ysbl.york.ac.uk/~cowtan/fourier/magic.html>

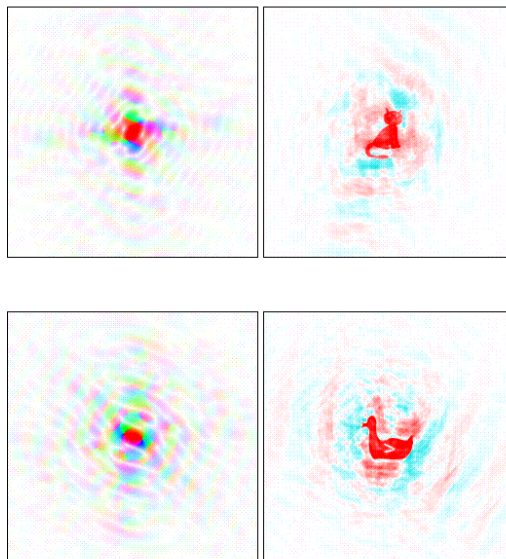


Figure 7: Illustrating the effect of amplitude and phase of visibilities in the image plane, namely that the phase describes the source structure and position. Top left, the fourier transformed image composed of the amplitudes of the duck and the phases of the cat. Inverse Fourier transform this and we get the image on the top right. Similarly for the bottom panels, this time using the phases of the duck and the amplitudes of the cat. Image Credit Keith Cowtan <http://www.ysbl.york.ac.uk/~cowtan/fourier/magic.html>

## 4 The Radio Interferometry Problem: The Classical View

In this next section, I will give a more rigorous summary of the 'classical' radio interferometry problem, the first principles behind the major interferometers in use today, such as the VLA, GMRT, WSRT and ATCA. Figure 8a) illustrates the basic problem we want to solve. How do we relate the signal measured by the interferometer, to the full electric field distribution on the sky? Detailed coverage of the underlying physics is given in many widely available texts, for example Thompson.(1986), Taylor.(1999),

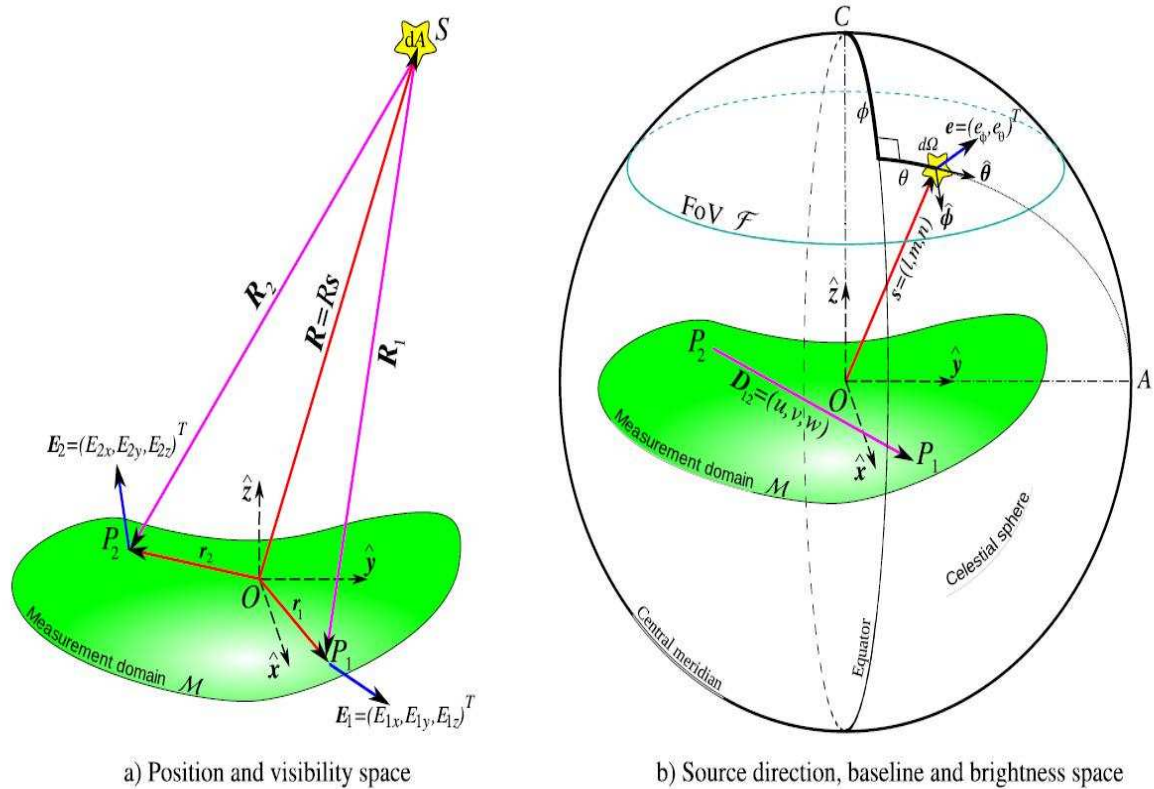


Figure 8: The Radio Interferometry Problem Illustrated. a) illustrates the basic problem, whereby an astronomical source emits radiation, and a time variable electric field  $\mathbf{E}(\mathbf{R},t)$  is measured at two different points in domain  $\mathcal{M}$ .  $O$  denotes the origin of the coordinate system used. b) Denotes the common coordinate system used in interferometric measurements. Image Credit: (Carozzi and Woan, 2008)

and Rohlfs.(2000) and I utilise these to compile a summary of the principles of radio interferometry relevant to this seminar. <sup>2</sup>. In order to simplify the theoretical background and give a more concise introduction, I introduce some simplifying assumptions, following a similar approach to Chapter 1, in Taylor.(1999).

- The Electric field  $\mathbf{E}$  is non time varying over short intervals. This will be generally true for most astrophysical sources of interest, e.g. supernova remnants, radio galaxies in which the signal does not vary over observational timescales of hours, but obviously not so for highly variable sources such as pulsars. However it allows the basic physical concepts to be illustrated.
- Polarisation is ignored, and therefore the measured electric field is treated as a scalar quantity, again for simplification.
- The sources of interest are so far away as to be only measurable in two dimensions, or their 'surface brightness'.
- The space in between the source and the observer is empty, and that therefore the propagation of the Electric field through the vacuum is linear and can be described by Maxwell's equations in a vacuum.

<sup>2</sup>I would also like to acknowledge here the presentations and notes obtained from a summer school in Synthesis Imaging, held at ATNF Narrabri in October 2008, which were very helpful in aiding my understanding of radio interferometry and were invaluable in explaining some of the key concepts presented here

Classic electromagnetism theory gives the form of an electric field in a vacuum as

$$E(t) = \int_0^{\infty} E(\nu) e^{i[\phi(\nu) - 2\pi\nu t]} d\nu \quad (2)$$

If the coefficient  $E(\nu)$  has a form which limits the range of frequency to an interval  $\delta\nu$  such that

$$\delta\nu/\bar{\nu} \ll 1 \quad (3)$$

where  $\bar{\nu}$  is the mean frequency then the signal is said to be quasi-monochromatic (K. Rohlfs, 2000), which is what is measured in reality, a signal over some small but finite bandwidth. So, applying the no short term time variability assumption to the quasi-monochromatic measurement of the electric field emitted by our source,  $\mathbf{E}(\mathbf{R}, t)$ , it is possible to express the electric field as Fourier series and utilise only the Fourier coefficients, rather than the full time varying wavefunction, as representative of the electric field at  $\mathbf{R}$ ,  $\mathbf{E}_\nu(\mathbf{R})$ .

Maxwell's equations for radiation propagating in a vacuum allow the determination of the electric field at location  $\mathbf{r}$ , in the form of a Green's function solution

$$\mathbf{E}_\nu(\mathbf{r}) = \int \int \int P_\nu(\mathbf{R}, \mathbf{r}) \mathbf{E}_\nu(\mathbf{R}) dx dy dz \quad (4)$$

where  $P_\nu(\mathbf{R}, \mathbf{r})$  is the propagator function which indicates how the source electric field affects the electric field measured at  $\mathbf{r}$ . By considering the electric field as a scalar, or in only one direction, this equation is simplified, and the assumption that that the space between the observer and source is empty is also applied. We also need to consider that the sources observed are so far away, that we can only make surface brightness measurements. For this reason, Taylor et al (1999) define a third electric field,  $\varepsilon_\nu(\mathbf{R})$ , as the electric field distribution on a giant celestial sphere of radius the absolute magnitude of  $\mathbf{R}$ . This gives us that the electric field measured at  $\mathbf{r}$  is,

$$E_\nu(\mathbf{r}) = \int \varepsilon_\nu(\mathbf{R}) \frac{e^{2\pi i\nu|\mathbf{R}-\mathbf{r}|/c}}{|\mathbf{R}-\mathbf{r}|} dS \quad (5)$$

where  $dS$  is an element of surface area on the celestial sphere. This is then the electric field measured by the observer at  $\mathbf{r}$  due to all sources of cosmic electromagnetic radiation.

## 5 Spatial Coherence

The simplest two element interferometer, see figure 9, measures the voltage induced by the electric field at two points,  $\mathbf{r}_1$  and  $\mathbf{r}_2$ , and then proceeds to correlate the signals. The correlation is defined as the expectation value of the product of the two electric fields:

$$V_\nu(\mathbf{r}_1, \mathbf{r}_2) = \langle \mathbf{E}_\nu(\mathbf{r}_1) \mathbf{E}_\nu^*(\mathbf{r}_2) \rangle \quad (6)$$

Substituting in equation 5, writing  $\mathbf{s} = \mathbf{R}/\|\mathbf{R}\|$ , and  $I_\nu(\mathbf{s})$  for the observed intensity and finally making the assumption that the radiation from two different points of the source is uncorrelated, the following expression, the spatial coherence function, is obtained:

$$V_\nu(\mathbf{r}_1, \mathbf{r}_2) \sim \int I_\nu(\mathbf{s}) e^{-2\pi i\nu \mathbf{s} \cdot (\mathbf{r}_1 - \mathbf{r}_2)/c} d\Omega \quad (7)$$

This quantity is what a single baseline of an interferometer measures (via induced voltages), and is invertible, in other words, given the spatial coherence function, we can obtain the observed intensity.

Choosing a set of coordinates wisely means that the spatial coherence function may be written in the form of a Fourier transform. If the coordinate system is chosen to be in a plane, we can write the separation vector in terms of the wavelength  $\mathbf{r}_1 - \mathbf{r}_2 = \lambda(u, v, w)$ , with the components of  $\mathbf{s}$  as  $(l, m, \sqrt{1 - l^2 - m^2})$ . Rewriting the coherence function in this coordinate system shows that the coherence function  $V_\nu(u, v, w=0)$  and the modified intensity  $I_\nu(l, m)/\sqrt{1 - l^2 - m^2}$  are a Fourier transform pair.

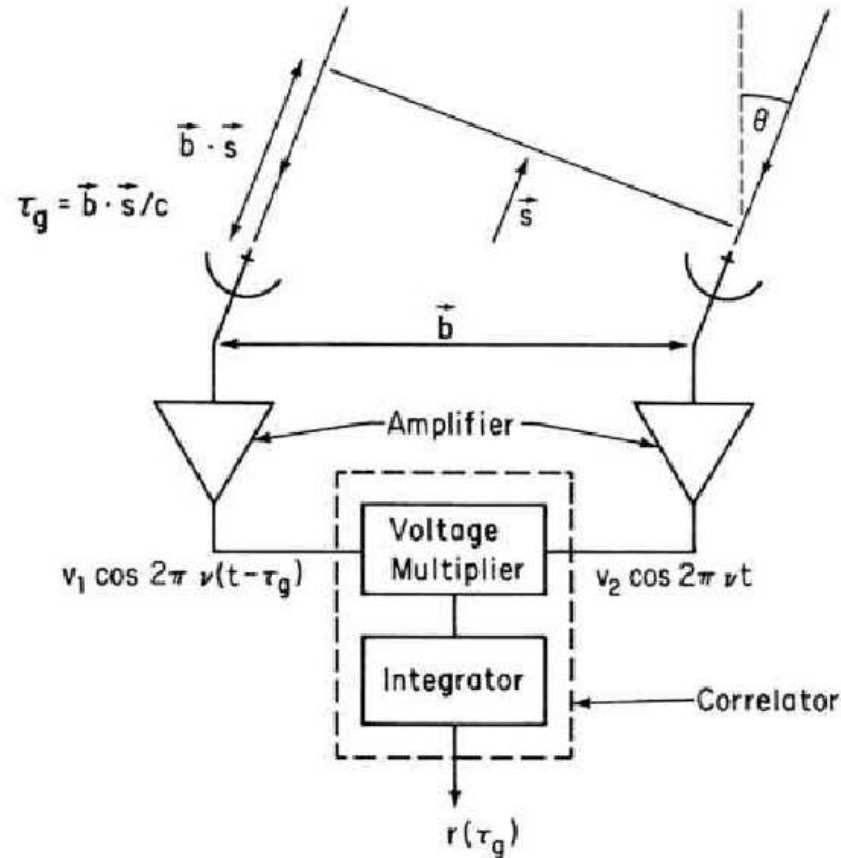


Figure 9: A Simple Two Element Interferometer. As shown by the figure, a wavefront from a source will arrive at a different time at each of the antennas. A correction is applied by the receivers for this geometrical delay. Image Credit: (Thompson, 1986)

If we then assume that we are looking at a small portion of the sky, in other words, a particular source, we can write  $\mathbf{s} = \mathbf{s}_0 + \sigma$ , where  $\mathbf{s}_0$  points from the antenna to the ‘phase tracking centre’, with the vector  $\sigma$  describing all nearby points on the sky, perpendicular to  $\mathbf{s}_0$ . This gives;

$$V_\nu(u, v) = \iint I_\nu(l, m) e^{-2\pi i(ul + vm)} dl dm \quad (8)$$

If geometrical delays are accounted for, see figure 9, then any phase difference relative to the phase tracking centre measured by the interferometer will be due to light from different parts of the source reaching the antennas at different times, giving a fringe pattern, and allowing source positions to be measured.

## 5.1 Aperture Synthesis

Each visibility measured is unique to a particular baseline length and orientation. In order to sample the entire  $u$ - $v$  plane in the most uniform way, we require as many different baselines lengths and orientation with respect to the sky as possible. Aperture synthesis is the process by which we take advantage of the Earth’s rotation to change orientations of baselines with respect to the sky, and hence sample the  $u$ - $v$  plane more completely, as illustrated in figure 10.

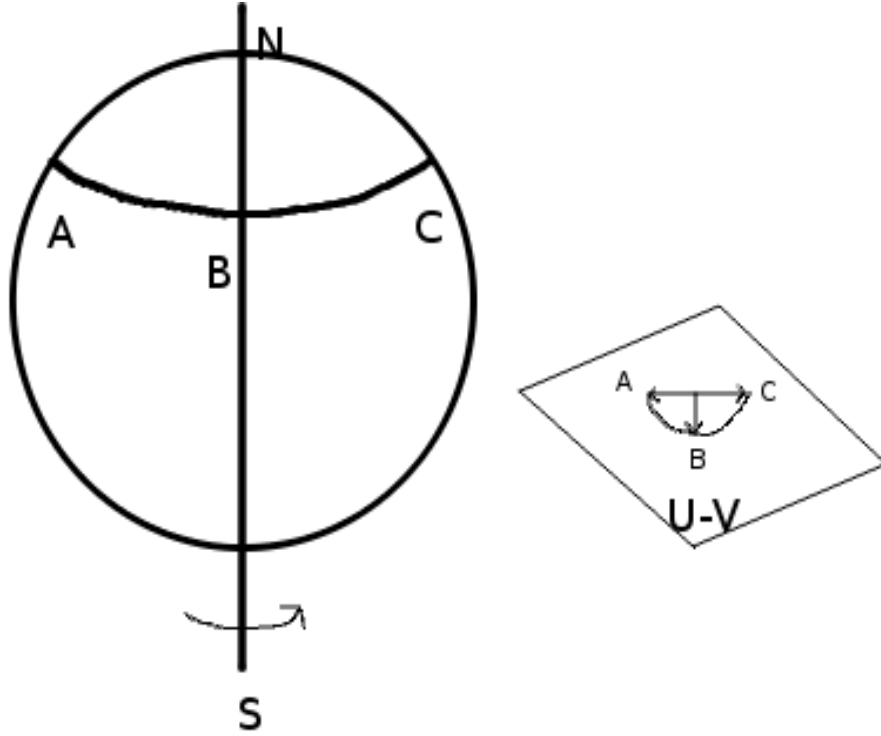


Figure 10: Aperture Synthesis Illustrated. This simple diagram illustrates how the U-V plane is sampled as the Earth rotates. Figure based on one included in the GMRT LFRA notes, available online at [http://gmrt.ncra.tifr.res.in/gmrt\\_hpage/Users/doc/WEBLF/LFRA/](http://gmrt.ncra.tifr.res.in/gmrt_hpage/Users/doc/WEBLF/LFRA/)

## 5.2 Primary Beam

In practice, two other effects must be accounted for when measuring the spatial coherence function  $V$ . Firstly the antenna reception pattern, or ‘primary beam’. This is a factor  $A_\nu(\mathbf{s})$  which effectively describes the sensitivity of the interferometer element with radius from the centre of the dish beam. The expression for spatial coherence then becomes;

$$V_\nu(u, v) = \int \int A_\nu(l, m) I_\nu(l, m) e^{-2\pi i(ul+vm)} dl dm \quad (9)$$

$V_\nu(u, v)$  defined in this way is referred to as a *visibility*. It is then straightforward to correct for this effect at later stages of data processing, when deriving the intensities, if all the interferometer elements have the same reception pattern. It is simply a case of dividing the measured intensities by a primary beam factor, approximately 1 at the phase tracking centre, and falling to smaller factors towards the outer edges of the beam.

## 5.3 Deconvolution

Secondly, in practice  $V_\nu(u, v)$  cannot be sampled everywhere in the uv plane. This is described by a sampling function, which is zero at the points in the plane where no measurements have been taken. Including this and Fourier inverting the visibility measured by the interferometer gives;

$$I_\nu^D(l, m) = \int \int V_\nu(u, v) S(u, v) e^{-2\pi i(ul+vm)} du dv \quad (10)$$

The set of fourier inverted visibilities  $I_\nu^D(l, m)$  is referred to as the *dirty image*. To obtain the true set of intensity values  $I_\nu(l, m)$ , the synthesised beam  $B$  corresponding to the sampling function must be deconvolved from the true intensity distribution.

$$I_\nu^D(l, m) = I_\nu * B \quad (11)$$

where  $B$  is the synthesised beam, related to the sampling function by;

$$B(l, m) = \int \int S(u, v) e^{2\pi i(ul+vm)} dudv \quad (12)$$

Deconvolution is generally carried out using the ‘CLEAN’ algorithm. Since  $I_\nu(l, m)$  cannot be recovered directly, due to the finite number of  $uv$  data points, the basic premise of ‘Clean’ is to assume that the image can be represented by a field of point sources. The algorithm then proceeds to find the point of highest intensity in the ‘Dirty’ image, and then subtract from the dirty image at this position, the intensity multiplied by the synthesised beam. Then repeat this process down to a peak intensity level specified by the user. Finally, it takes the accumulated point source model, and convolves it with an idealised synthesised beam (usually a gaussian fitted to central lobe of the synthesised beam), then adds the residuals of the dirty image to this image. <sup>3</sup>.

Thus in order to make an image of the true intensities, the spatial coherence function must be measured with good coverage in the  $uv$  plane by the interferometer and these visibilities then fourier inverted, and the synthesised beam deconvolved.

## 6 Calibration and Editing

Taking a step back, in practice, the observed visibilities will differ from the true visibilities due to a less than perfect instrument, and a variety of additional mechanisms, for example refraction by the ionosphere. Estimating these effects, and correcting the observed visibilities to obtain the true visibilities is the process known as calibration.

Editing, or ‘flagging’ refers to the process of excluding data that is severely corrupted. This can be due to instrument problems, bad weather, interference from man-made sources etc. Generally all radio interferometric observations will require some flagging.

Formally, for one baseline with antennas  $i$  and  $j$  we can define a relation between the observed visibilities  $\tilde{V}_{ij}(t)$  and the true visibilities  $V_{ij}(t)$ .

$$\tilde{V}_{ij}(t) = \tilde{G}_{ij}(t)V_{ij}(t) + \epsilon_{ij}(t) + \eta_{ij}(t) \quad (13)$$

where  $t$  is the time of the observation,  $\tilde{G}_{ij}(t)$  is the baseline based complex gain,  $\epsilon_{ij}(t)$  is a baseline based complex offset, and  $\eta_{ij}(t)$  is a stochastic complex noise. The simplest way of performing a calibration is to use observations of a point source with known flux density  $S$ , and known position. The true visibility amplitude will be  $S$  Jy, and phase will be 0 (observing the calibrator in the centre of the field). Therefore the estimate of the gain is

$$\tilde{G}_{ij}(t)V_{ij}(t) = \frac{\tilde{V}_{ij}(t)}{S} \quad (14)$$

The offset terms  $\epsilon_{ij}(t)$  and  $\eta_{ij}(t)$  are assumed to be negligible after averaging of data in the scan. This is a simplified view of the scalar, total intensity case, and the process of calibration requires many more considerations. Some of these are looked at within the context of the Measurement Equation in section 9, but for more detail, see Taylor et al. (1999).

### 6.1 Self-Calibration

A detailed look at self-calibration is beyond the scope of this seminar, however it is an important step in the data reduction process. Self-calibration is the process of allowing the gains of each individual element to be a free parameter. This allows individual element instrumental & atmospheric effects to be corrected for. Self-calibration is possible as we have many antenna/station/dipole elements, and hence a large redundancy in the initial calibration. The process of self calibration is as follows. Starting with usually a CLEANed image of the field, this can be converted to a point source model and the gains solved for. The visibilities are corrected and a new image made. This cycle is repeated until the image shows no more visible improvement.

<sup>3</sup>For further details see ‘The Deconvolution Tutorial’, available online at <http://www.cv.nrao.edu/~abridle/deconvol/deconvol.html>

## 7 In Practice

Traditional interferometric imaging packages such as AIPS or MIRIAD will perform the steps described above through a variety of 'tasks'. CASA, a next generation package is similar in nomenclature to AIPS.

- Raw uv-data - tasks to plot the raw visibilities. Editing tasks to 'flag' or exclude RFI (Radio frequency interference, eg local radio station signals etc).
- Raw uv-data calibration - tasks to utilise known sources to calibrate the raw visibilities.
- The dirty image - imaging task to inverse fourier transform the calibrated visibilities.
- deconvolution - imaging task implementing the 'CLEAN' algorithm to deconvolve the synthesised beam from the image

## 8 The Measurement Equation

The basic concepts which I have presented so far are standard as an introduction to radio astronomy, and are described in far greater detail in the classic texts of Thompson.(1986) and Taylor.(1999). This is the standard layout which underpins many of the major existing software packages such as AIPS, MIRIAD etc. Do we need to do better?

- we do not have a full mathematical description of the polarisation.
- the assumptions above are much more difficult to implement for an array of dipoles, with a field of view covering the whole sky.
- existing calibration corrects uv-plane effects: there is no allowance for correction of image plane effects, such as ionospheric variations.
- existing packages are difficult to add to/modify, and are no longer being actively maintained.

In 1996 Hamaker et al derived a mathematically complete description of what is measured by any interferometer.<sup>4</sup> The measurement equation effectively describes the path of the radio signal through the various propagation mediums, such as the ionosphere, antenna feeds etc up until reception by the correlator, by a series of matrices, the Jones matrices.

The field of optical polarimetry has a wide range of formalisms available to describe polarisation. We have the Stokes parameters to describe the state of polarisation of light, and the Jones and Mueller matrices to describe the transformation of the polarisation state as the wave propagates through various mediums. As a reminder Mueller matrices are a generalisation of the Jones matrices. Jones matrices are only applicable to fully polarised light.

The Measurement Equation provides a transparent and compact description of radio interferometric measurements at all polarisations, and is being adopted as the formalism in new interferometric reduction packages intended for telescopes such as LOFAR and the SKA. See for example the AIPS++/CASA cookbook, or the guide to Meqtrees Noordam(2009), a calibration and simulation package for LOFAR.

Beginning with the assumption that all the radiation arrives from a single point, the propagation of the 'source' electric field is defined as

$$\mathbf{e} = \begin{pmatrix} e_x \\ e_y \end{pmatrix}$$

(15)

in the xy plane, with z the direction of propagation.

<sup>4</sup>See Taylor.(1999), chapter 32 for a detailed introduction. The simple derivation I give here is based on the lectures by Oleg Smirnov & Jan Noordam at MCCT SKADS 2009

The Measurement Equation formulation makes only one main assumption, that the propagation of the wave is *linear*. Therefore this propagation can be described by a 2x2 matrix, and the voltages measured by each antenna, or station are also linear with respect to  $\mathbf{e}$ .

$$\mathbf{v} = \mathbf{J}\mathbf{e} \quad (16)$$

Returning to the simplest two element interferometer, antennas/stations p and q measure voltages described by

$$\mathbf{v}_p = \mathbf{J}_p\mathbf{e} \quad (17)$$

$$\mathbf{v}_q = \mathbf{J}_q\mathbf{e} \quad (18)$$

The interferometer measures the cross correlations between the two voltages.

$$v_{xx} = \langle v_{px}v_{qx}^* \rangle \quad (19)$$

$$v_{xy} = \langle v_{px}v_{qy}^* \rangle \quad (20)$$

$$v_{yx} = \langle v_{py}v_{qx}^* \rangle \quad (21)$$

$$v_{yy} = \langle v_{py}v_{qy}^* \rangle \quad (22)$$

Writing these as a matrix product

$$\mathbf{V}_{pq} = \left\langle \begin{pmatrix} v_{px} \\ v_{py} \end{pmatrix} (v_{qx}^* v_{qy}^*) \right\rangle = \begin{pmatrix} v_{xx} & v_{xy} \\ v_{yx} & v_{yy} \end{pmatrix} \quad (23)$$

This is known as the *visibility* matrix. Substituting in the expressions above

$$\mathbf{V}_{pq} = \langle (\mathbf{J}_p\mathbf{e})(\mathbf{J}_q\mathbf{e})^T \rangle = \langle \mathbf{J}_p(\mathbf{e}\mathbf{e}^T)\mathbf{J}_q^T \rangle = \mathbf{J}_p\langle \mathbf{e}\mathbf{e}^T \rangle\mathbf{J}_q^T \quad (24)$$

The inner quantity is known as the source coherency, or source brightness, and can be written in the more familiar terms of the Stokes parameters as

$$\mathbf{B} = \langle \mathbf{e}\mathbf{e}^T \rangle = 0.5 \begin{pmatrix} I + Q & U \pm iV \\ U \pm iV & I - Q \end{pmatrix} \quad (25)$$

Finally we can write

$$\mathbf{V}_{pq} = \mathbf{J}_p\mathbf{B}\mathbf{J}_q^T \quad (26)$$

which is the measurement equation. The  $\mathbf{J}$ s are known as Jones matrices, and they are a product of individual Jones terms, describing the full signal path. The order of the  $\mathbf{J}$ s is important, it follows the physical order of effects in your signal path, reading right to left in the equation.

The majority of physical effects on the signal path have a simple Jones matrix representation, for example a Faraday Rotation term would appear as

$$\mathbf{F} = (RM/\nu^2) \begin{pmatrix} \cos\theta & -\sin\theta \\ \sin\theta & \cos\theta \end{pmatrix} \quad (27)$$

The generic Jones terms can be listed as

$$J_i = G_i [H_i] [Y_i] B_i K_i T_i F_i = G_i [H_i] [Y_i] (D_i E_i P_i) K_i T_i F_i \quad (28)$$

in which

$F_i(\vec{\rho}, \vec{r}_i)$	ionospheric Faraday rotation - the polarisation plane of the wave is rotated after passing through ionosphere.
$T_i(\vec{\rho}, \vec{r}_i)$	atmospheric complex gain - refraction/extinction by atmosphere.
$K_i(\vec{\rho}, \vec{r}_i)$	factored Fourier Transform kernel - needed for modelling a tied array.
$P_i$	projected <i>receptor</i> orientation(s) w.r.t. the sky, or parallactic angle term
$E_i(\vec{\rho})$	voltage primary beam
$D_i$	position-independent <i>receptor</i> cross-leakage - how much radiation is picked up by one receptor that should be picked up by the other.
$[Y_i]$	commutation of <i>IF-channels</i>
$[H_i]$	hybrid (conversion to circular polarisation coordinates)
$G_i$	electronic complex gain ( <i>feed</i> -based contributions only)

Matrices between brackets ([ ]) are not present in all systems.  $B_i$  is the ‘Total Voltage Pattern’ of an arbitrary *feed*, which is usually split up into three sub-matrices:  $D_i E_i P_i$ . Jones matrices that model ‘image-plane’ effects depend on the source position (direction)  $\vec{\rho}$ . Some also depend on the antenna position  $\vec{r}_i$ , and most on time and frequency as well<sup>5</sup>, see Noordam. (Noordam, 1996).

*In general, these matrices do not commute, so the order is key.*

This is an important point, as in many of the older packages, several effects are often grouped together, when they do not necessarily commute.

For example parallactic angle and ionospheric Faraday rotation come after primary beam, as they do not commute with the primary beam matrix, yet the Faraday rotation matrix is often combined with the receiver gain term. This is also the case for tropospheric effects, which are also often included as part of the receiver gain term. Conversely, grouping several effects together can give substantial gains in computational efficiency. This leads to the obvious question, why does existing calibration apparently work so well?

The answer lies in the fact that several of these effects can be approximated by matrices that do commute with some others whilst in the wrong order. These approximations are good for existing arrays, but will not in general apply to newer ones.

As an example, let’s look at the ionosphere. Often Faraday rotation and atmospheric complex gain are included as part of the receiver gain. This is an acceptable approximation for most existing arrays where the ionosphere TEC (total electron content) does not change noticeably over the primary beam (field of view of antenna), and there is no appreciable cross-leakage. This however will be a significant effect for new dipole arrays, see figure 11, as the field of view of each dipole is so large as to see a changing ionosphere, and a cross-leakage term will be necessary.

This seems very intuitive, so why has the full measurement equation not been implemented until now? Most older existing packages use some implicit, specific to the instrument, form of the measurement equation, and work well for current, well understood instruments such as the VLA and WSRT. However even the most widely used packages such as AIPS are no longer being actively developed, and are difficult to modify. Re-writing AIPS is not practical (or indeed necessary for existing instrument data analysis)! For the next generation of radio telescopes, the Measurement Equation is not just an elegant formalism, but a requirement, to enable good calibration of polarisation and ionospheric effects.

---

<sup>5</sup>Jan Noordam’s latex file of Measurement Equation notation was used in preparing this lecture, available online at <http://www.astron.nl/~noordam/>.

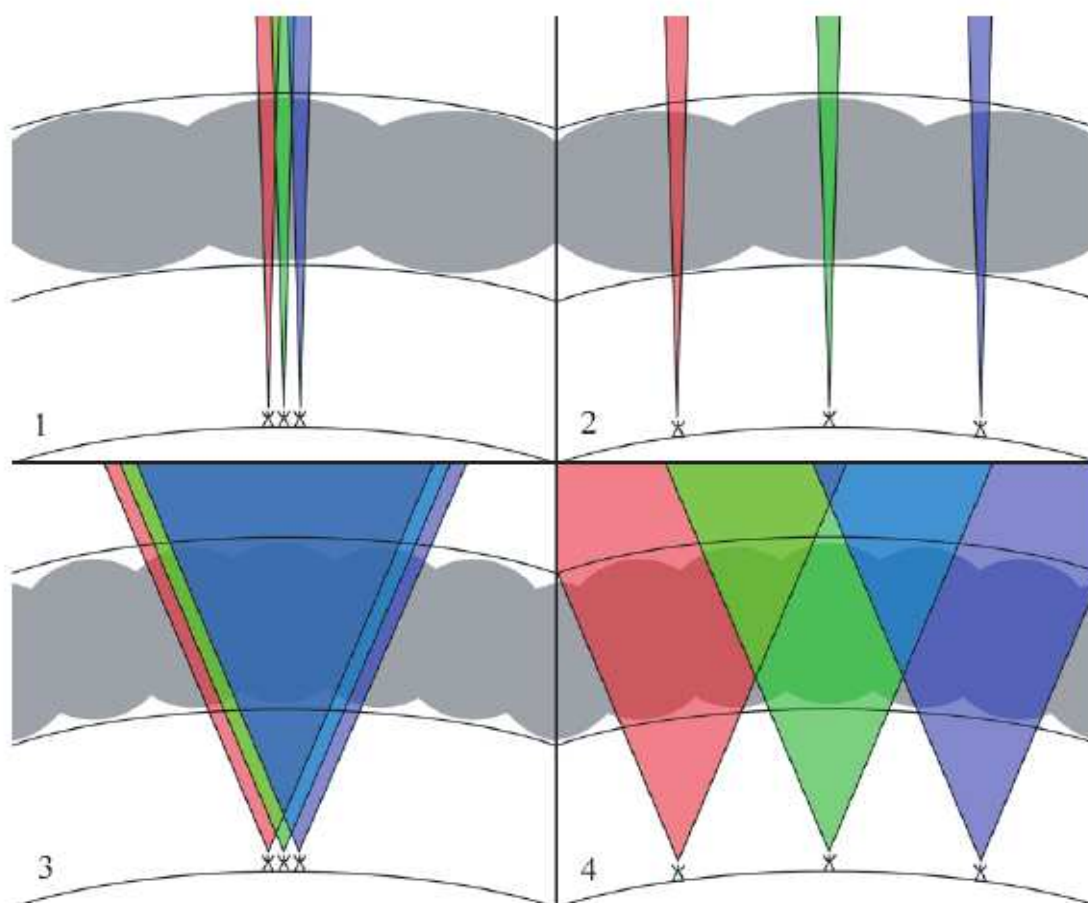


Figure 11: Effect of the Ionospheric TEC on Different Arrays. Panels one and two show array elements with narrow fields of view - each element will see an approximately constant TEC. In panels three and four, the wide field of view of the elements imply that each element will see a changing TEC across the field of view. For the compact array illustrated in panels one and three, the variation in the ionospheric TEC for a particular viewing direction in the field of view will be a gradient, however for the extended arrays in two and four, this will not be the case. For panels one and two, traditional self calibration is sufficient to correct the ionospheric effects. However in panels three and four, the ionosphere changes with both time and viewing direction, and more advanced calibration methods are required, such as SPAM, Intema et al. (2009).

## References

- Carozzi, T. D. and Woan, G.: 2008  
 G.B. Taylor, C.L. Carilli, R. P. (ed.): 1999, *Synthesis Imaging in Radio Astronomy II*, Vol. 180, Astronomical Society of the Pacific Conference Series  
 Hamaker, J. P., Bregman, J. D., and Sault, R. J.: 1996, **117**, 137  
 Intema, H. T., van der Tol, S., Cotton, W. D., Cohen, A. S., van Bemmell, I. M., and Rottgering, H. J. A.: 2009  
 Jackson, N.: 2004, *Principles of Interferometry*  
 K. Rohlfs, T. W.: 2000, *Tools of Radio Astronomy*, Astronomy and Astrophysics Library, Springer  
 Noordam, J.: 1996, *The Measurement Equation of a Generic Radio Telescope*, Technical report, ASTRON, NFRA  
 Noordam, J.E. Smirnov, O.: 2009, *Megtrees: A Software Module for Implementing an Arbitrary Measurement Equation and Solving for its Parameters*, Project Documentation Version 0.991, ASTRON, Dwingeloo  
 Thompson, A.R. Moran James M. Swenson, G. W.: 1986, *Interferometry and Synthesis in Radio*

*Astronomy*, John Wiley & Sons, Inc.  
Zhao, G.: 2009, in *Bulletin of the American Astronomical Society*, Vol. 41 of *Bulletin of the American Astronomical Society*, pp 405–+